Effect of starch nanocrystals on natural rubber latex vulcanizate properties

Anand K[1,], Siby Varghese[2], Thomas Kurian[3] and Suryasarathi Bose[4]*

[1]Department of Basic Sciences, Amal Jyothi College of Engineering, Kanjirappally, Kerala 686 518, India
[2]Technical Consultancy Division, Rubber Research Institute of India, Kottayam, Kerala 686 009, India
[3]Department of Polymer Science and Rubber Technology, Cochin University of Science and Technology, Kochi 682 022, India
[4]Department of Materials Engineering, Indian Institute of Science, Bangalore 560 012, India

Received: 9th October 2016, Accepted: 8th March 2017

SUMMARY

The incorporation of bio-nanofillers such as starch nanocrystals (SNC) in polymer matrices received much attention owing to their biodegradable nature. In this work, starch nanocrystals have been isolated from modified corn starch by acid hydrolysis and their efficacy as a potential bio-filler for natural rubber latex (NR) has been explored. The quality of the SNC suspension was confirmed from dynamic light scattering (DLS) studies and X-ray diffraction (XRD) measurements. For the fabrication of nanocomposites of NR with corn starch crystals, a simple latex stage mixing procedure was employed. The platelet-like morphology of corn starch nanocrystals improved the barrier properties of NR based vulcanizates with the addition of the SNC suspension.

Keywords: Corn starch; Starch nanocrystals; XRD; SEM; Swelling; Mechanical properties

INTRODUCTION

Starch is a naturally occurring biodegradable polysaccharide produced by almost all green plants and is a major source of energy in the world of flora. It

*Corresponding author
E-mail: anand.rrii@gmail.com

is the second most abundant biomass material in nature and found abundantly in plant roots, stalks, crop seeds and staple crops such as rice, corn, wheat, tapioca and potato [1,2]. Starch is composed of two polysaccharides, amylose and amylopectin, whereas, glucose units are joined by glycosidic bonds. The amorphous (amylose) and crystalline (amylopectin) components of native starch granules are arranged alternatively encircling the point of initiation known as hilum [3].

The total worldwide starch utilization in 2008 was 66 million tons, with US being the largest starch manufacturer with bioethanol and fructose syrups together totalling 72% of starch output [4]. The modified starch output is expected to experience a growth of 4.1% in 2013–2018. In India, NPCS estimates that the production of starch and its derivatives was 970000 tonnes in 2010 and is anticipated to reach 2749000 tonnes by the year 2017 [5]. Low density, cost-effectiveness, environmental safety and abundant supply of these materials demand applications in various industries.

Starch nanocrystals (SNC) are formed as distinct crystalline platelets due to the disruption of the semi-crystalline structure of starch granules by the acid hydrolysis of amorphous parts [6]. Acid hydrolysis for the isolation of SNCs is cumbersome process due to several factors, such as time of hydrolysis, concentration and type of acid used, temperature *etc.* Therefore, proper control over these parameters is crucial for the fabrication of starch nanoplatelets. The distinct platelet-like morphology, strong interfacial interaction and rigidity of the starch nanocrystal ensure improved mechanical performance, reduced solvent penetration and improved barrier properties when incorporated into a polymer matrix.

With increasing environmental awareness, replacement of conventional non-renewable inorganic fillers like clay, silica *etc.* with eco-friendly bio-fillers like starch, cellulose *etc.* is getting wide acceptance for various industrial applications, particularly in rubber and allied industries where fillers are essential for improved product performance. It is also possible to develop novel functional materials with the incorporation of suitable nanofillers. Goodyear Tire and Rubber (USA) has recently developed tyres with a 30 per cent reduction in rolling resistance. They used nanoparticles derived from corn starch for partial replacement of carbon black and silica. Goodyear has been working on the corn starch-based filler since the mid-1990s and launched a tire, the GT3 BioTread, in 1999 [7].

The structural and mechanical properties of natural rubber latex filled with starch nanocrystals extracted from different sources were investigated before [8]. Waxy maize starch nanocrystals (2-50 wt.%) were incorporated into a natural rubber latex matrix and the properties of the nanocomposites such as morphology, crystallinity, swelling behaviour, barrier properties for water vapour and oxygen, thermal properties and mechanical properties were investigated [9]. The effect of moisture content and surface chemical modification of the starch nanocrystals on the reinforcing properties of natural rubber was investigated

[10]. Tang *et al.* used different modifying agents to improve the interaction of starch with SBR and studied the curing behaviour, thermal and mechanical properties of the rubber compounds [11].

In the present study, we have isolated starch nanocrystals from modified corn starch and investigated their effect on natural rubber latex vulcanizate properties. The morphology and microstructure of the isolated corn starch nanocrystals are also studied. Finally, the mechanical properties of the composites obtained from the experimental results are compared with theoretical predictions.

MATERIALS AND METHODS

Modified corn starch was supplied by Jemsons starch and derivatives, Aroor, Kerala, India. Concentrated H_2SO_4 (98.08%) used was of LR grade supplied by NICE chemicals, Kochi, India. Centrifuged high ammonia latex was collected from Central Experimental Station of the Rubber Research Institute of India. Other compounding ingredients used were purchased commercially and aqueous dispersions were made by ball milling.

Preparation of starch nanocrystals

Corn starch nanocrystals were isolated from modified corn starch by acid hydrolysis. Characteristics of modified corn starch are given in **Table 1**. 120 g Modified corn starch were mixed with 816 ml 3.16 M conc. H_2SO_4 using a magnetic stirrer in a water bath maintained at 45°C for 5 days. The resultant aqueous suspension was centrifuged at 10000 rpm for 15 min. and washed several times with distilled water until neutrality (pH = 7). The supernatant solution was discarded and the gel like precipitate thus obtained scooped off and collected. The solid fraction of the suspension had a concentration of about 11.8 per cent. The resulting suspension was sonicated for about 10 min and a portion of it was used for DLS and XRD analyses.

Characterization

Wide angle and small angle 2D-X-ray scattering were measured using Xeuss simultaneous WAXS/SAXS instruments. Cu-Kα was the X-ray source with a

Table 1 Characteristics of modified corn starch

Appearance	Pale white powder
Moisture	6%
pH	12.4
Solubility	Fully soluble

Table 2 Formulation of the mixes

Ingredients	Dry weight (phr)
60% Centrifuged latex (High ammonia type)	100
10% Potassium hydroxide solution	0.3
50% Sulphur dispersion	1.5
50% ZDC* dispersion	1
50% ZnO# dispersion	0.4
30% Wingstay (A/O) dispersion	0.75
Corn starch suspension	0 (gum), 0.69, 1.38, 2.75

*Zinc diethyldithiocarbamate.
#Zinc oxide.

collimated area of 0.64 mm^2. Silver behenate was used for distance calibration. 2D- X-ray scattering data were azimuthally integrated using Fit-2D software. The hydrolyzed starch samples were placed in a sample holder for X-ray measurements. The crystallinity of the corn starch nanocrystals was calculated using the method described elsewhere [12]. Scanning Electron Microscopy (SEM) analysis of hydrolyzed sample was performed using ZEISS EVO 18 Cryo SEM special edition with variable pressure working at 15–30 kV. The sample was prepared by the drop casting method on a carbon tape.

Composite preparation

Corn starch crystal suspensions were mixed well with compounded natural rubber latex at various proportions (0.69, 1.38 and 2.75 phr) and films were casted at room temperature and kept overnight. The formulation of the mixes is given in **Table 2**. The cast films were dried at 70°C for 2.5 h and then vulcanized at 105°C for 35 min.

Sorption studies

The kinetics of toluene absorption was determined for all the vulcanizates (gum, 0.69, 1.38 and 2.75 phr SNC incorporated). Circular specimens having uniform diameter were cut from the film and immersed in toluene up to 48 h. The solvent absorption was periodically monitored and the swelling index at these intervals was calculated using the equation:

$$Q\ (\%) = \frac{W_t - W_0}{W_0} \times 100$$

Where W_0 and W_t are the weight of the films before and after a time t of immersion.

The toluene uptake (TU %) and sorption coefficient (S) of composite samples were calculated using the equations [8]

$$TU\ (\%) = \frac{m_t - m_0}{M_w \times m_0} \times 100$$

$$S\ (\%) = \frac{M_\infty}{M_0} \times 100$$

where m_0 and m_t are the weights of the samples before and after time t and M_w is the molecular weight of toluene (92.14 $gmol^{-1}$). M_0 and M_∞ are the initial mass of the polymer film and mass of the solvent adsorbed at equilibrium.

Mechanical property measurements

Tensile pieces were punched from the cast films and were employed to measure the mechanical properties. Six replicates were used and the average value was considered. Tension set was measured as per IS 4148. Tensile specimens having 40 mm length and 0.6 mm width were punched out and extended up to five times to its length (200 mm) in Instron 4411 machine and kept for 10 minute. The samples were released and kept in a flat surface at room temperature for 10 min. to attain equilibrium and afterwards, the change in length was measured.

Leaching of the latex films were carried out in distilled water for about 4 h and then the films were dried and kept in a desiccator overnight. The mechanical properties were performed the next day.

The modulus of the composite films was predicted using the following theoretical models and compared with the experimental results [13–16].

Einstein equation

$$E' = E_0\,(1 + 2.5c) \tag{1}$$

Guth equation

$$E' = E_0\,(1 + 2.5c + 14.1c^2) \tag{2}$$

Brinkman equation

$$E' = E_0\,(1-c)^{-5/2} \tag{3}$$

Ponte Castaneda equation

$$E' = E_0 / (1-3c) \tag{4}$$

where E_0 and E′ represents modulus of gum and filled samples respectively and '*c*' indicates the filler fraction.

RESULTS AND DISCUSSION

The particle size (DLS) curves of native corn starch (modified) and acid hydrolysed (5 days) corn starch is displayed in **Figures 1(a)** and **1(b)**, respectively. The mean particle size (D50) of native corn starch was 31.9 μm and it reduced to 2.84 μm after acid hydrolysis. D50 represents the particle diameter below which 50 per cent of the sample volume exists. It is also known as Mass Median Diameter (MMD). Also, the specific surface area (SSA) of native corn starch (modified) was 238 m^2/kg only and it increased to 3035 m^2/kg after acid

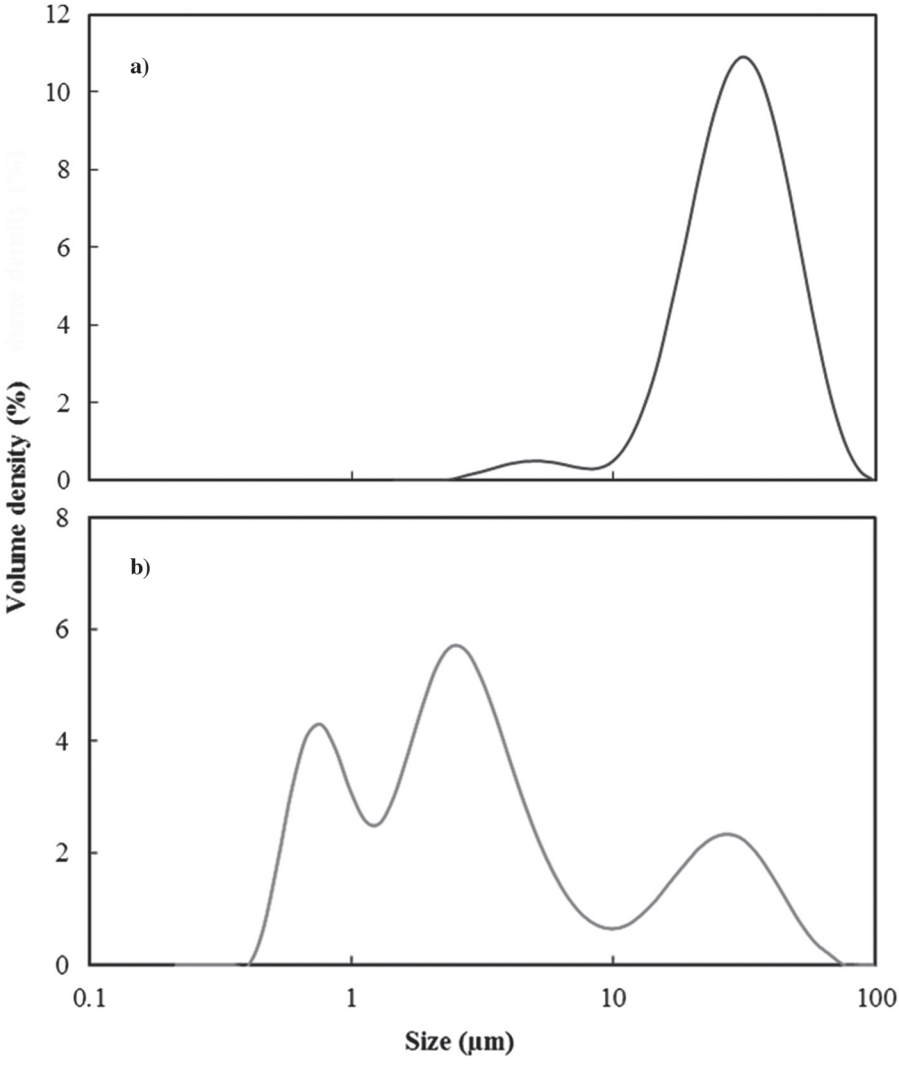

Figure 1 Size distribution curves of (a) native corn starch (modified) and (b) acid hydrolyzed corn starch

hydrolysis confirming the presence of corn starch nanocrystals. It is well known that smaller particles possess higher surface area. However, moderate agglomeration/flocculation of starch nanocrystals can also be seen from **Figure 1(b)**. This can be attributed to hydrogen bonding of smaller particles obtained after hydrolysis of partially hydrolyzed particles [17].

The XRD pattern of corn starch nanocrystals is shown in **Figure 2**. Hibi *et al.* studied the effect of high pressure on the crystalline structure of corn, rice and potato starch granules. They found that high pressure changed the A-type crystalline structure to B- type [18]. The strong peaks obtained at $2\theta=15^0$, 17^0, 17.9^0 and 22.9^0 confirms that the crystal structure is A-type. The results are in accordance with the earlier findings [19,20]. The peak at $2\theta=17^0$ is much more prominent than other peaks. The sharper peak obtained after hydrolysis indicates that the crystallinity of the starch increased and might be attributed to the hydrolysis of amorphous regions of starch granules. After 5 days of hydrolysis, the crystallinity index of the starch nanocrystal was 33.11 per cent.

The morphology of acid hydrolyzed (5 days) modified corn starch was observed by SEM and is shown in **Figure 3**. As revealed from the figure, an irregular platelet like crystalline morphology was observed for SNC. The surface was not smooth. The surface roughness and heterogeneity in shapes can be understood due to the adhesion between some starch granules and the surface erosion and fracture induced by continuous stirring [19]. Also, during acid treatment the starch granules undergo morphologic alterations [21].

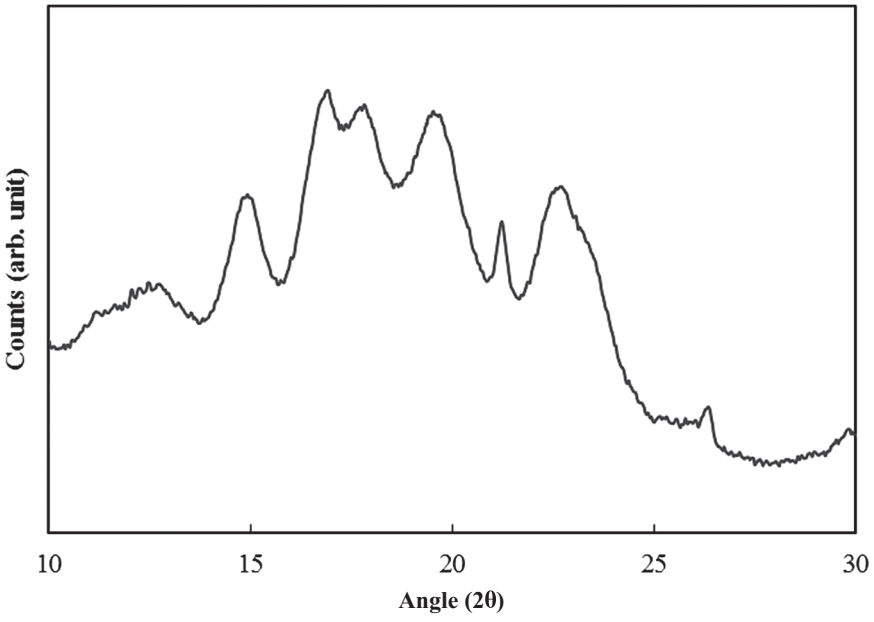

Figure 2 X-ray diffraction pattern of corn starch nanocrystals

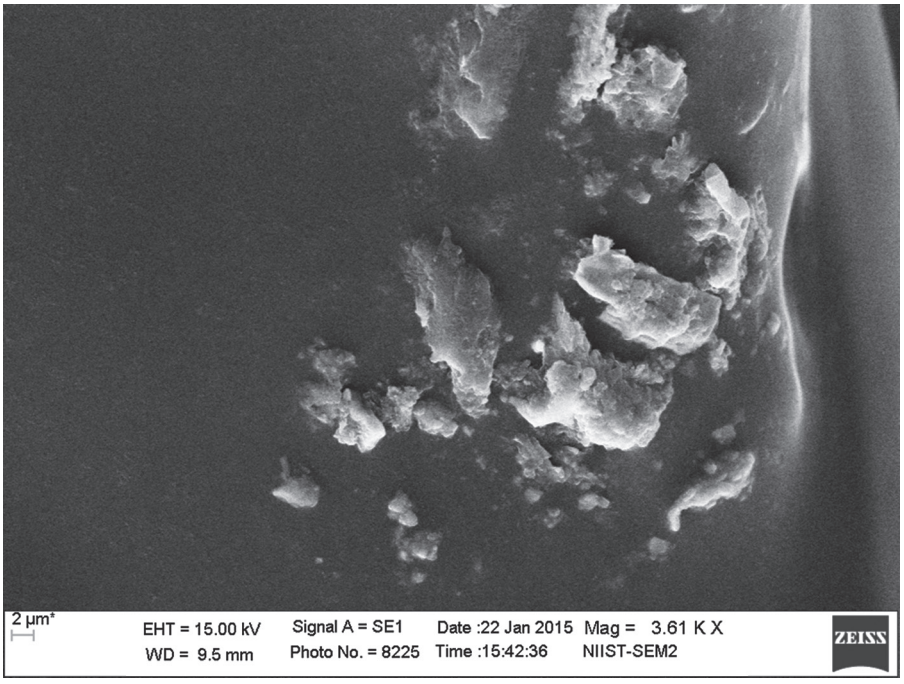

Figure 3 SEM image of modified corn starch granules after 5 days of acid hydrolysis

The swelling behaviour of the gum and starch nanocrystals filled vulcanizates (0.69, 1.38 and 2.75 phr) in toluene was evaluated and the swelling index (%) of vulcanizates as a function of square root of time is displayed in **Figure 4**. The swelling measurements were carried out up to 48 h ($\sqrt{t}$ =53.3 min) and equilibrium was considered to be reached at this immersion time. Initially, except for the 0.69 phr SNC incorporated system; the vulcanizates (gum, 1.38 and 2.75 phr SNC filled) exhibited a higher swelling index. However, after 48h, the swelling index of gum and 0.69 phr SNC filled systems were almost the same and are 435 and 433.3 respectively. The lowest swelling index of 422 was achieved by 1.38 phr SNC loading whereas it is slightly higher (425) for NR containing 2.75 phr SNC. The toluene uptake and sorption coefficient of gum and filled vulcanizates are given in **Table 3**. Here also, the lowest values were obtained for the 1.38 phr SNC loaded systems. The platelet like morphology and more uniform distribution of SNC in polymer matrix also offer reduced sorption and organic solvent uptake. The slight increase in toluene uptake and sorption coefficient for the highly filled systems (2.75 phr SNC loading) might be due agglomeration among starch nanocrystals.

The mechanical properties of gum and SNC filled vulcanizates (0.69, 1.38 and 2.75 phr) are given in **Table 4**. The reinforcing capability of SNC is evident from the modulus values. Modulus is a bulk property and it depends mainly on the geometry, particle size and distribution of the filler as well as the

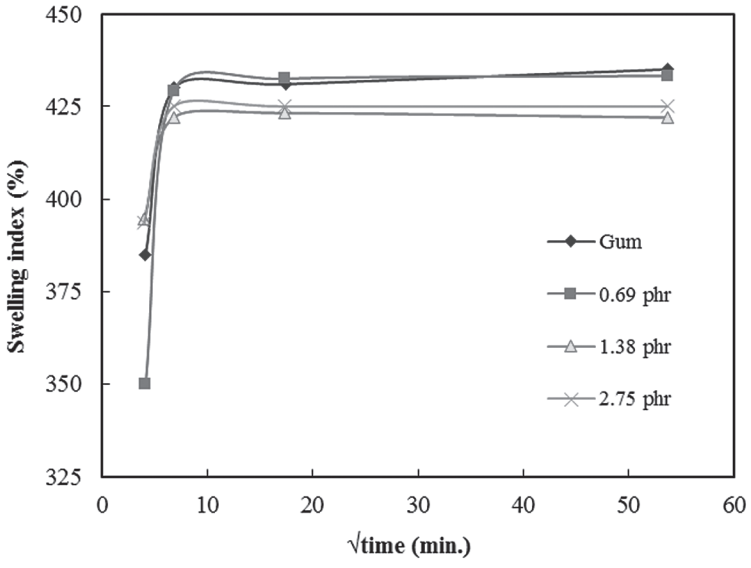

Figure 4 Swelling characteristics of SNC filled NR vulcanizates

Table 3 Toluene uptake and sorption coefficient of gum and filled vulcanizates

	Gum	CS 0.69	CS 1.38	CS 2.75
Toluene uptake (mol.%)	4.72	4.7	4.58	4.61
Sorption coefficient (%)	535	533	522	525

concentration of the filler. The monotonic increase in 500% modulus of NR vulcanizates with filler content can be ascribed to increased specific surface area (SSA) and aspect ratio resulting in high interaction between SNC and rubber matrix. Recently, it has been reported that, the addition of hydrolysed corn flour into natural rubber resulted 2 – 3 times increase in modulus when the filler content varies from 10 – 40 per cent [22].

The effect of leaching on the variation in tensile strength of the resulting vulcanizates (gum and filled) is shown in **Figure 5**. The leaching process was performed on most of the dipped products, threads and moulded foams to obtain improved properties. It is also crucial for medical goods and electrician gloves where the presence of hydrophilic materials would cause absorption of atmospheric moisture and consequently accounts for reduction in electrical resistance [23]. The leaching process gives rise to increased tensile strength and modulus values. As anticipated, after leaching, all the vulcanizates showed improved tensile strength, which is more pronounced in the filled systems. The tensile strength of gum and SNC filled vulcanizates (0.69, 1.38 and 2.75 phr loading) are 24.35 MPa, 23 MPa, 17.5 MPa and 19.8 MPa respectively (**Table 4**), and after leaching the values increased to 25.7 MPa, 26 MPa, 23.3 MPa and 21.8 MPa respectively.

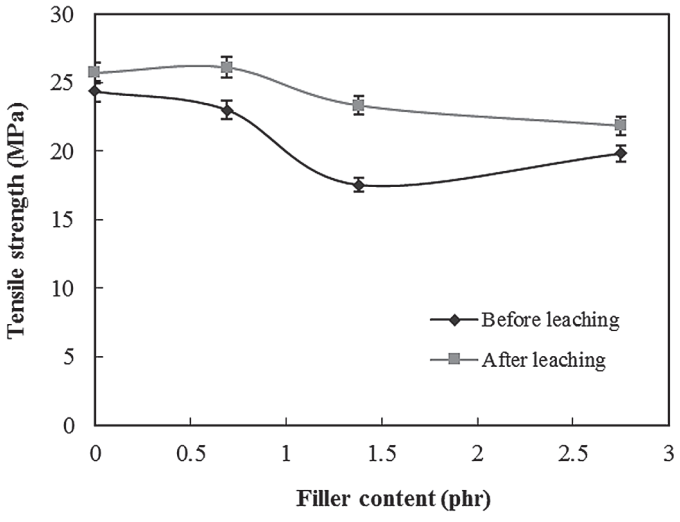

Figure 5 Tensile strength of SNC incorporated NR composites before and after leaching

Table 4 Mechanical properties of gum and filled vulcanizates

Properties	Gum	CS 0.69	CS 1.38	CS 2.75
Tensile strength (MPa)	24.35	23	17.53	19.82
Elongation at break (%)	1388	1399	1379	1246
100% modulus (MPa)	0.69	0.71	0.74	0.84
500% modulus (MPa)	1.74	1.7	1.87	2.33
Tension set	2.5	5	5	7.5

The improved tensile strength for filled latex films after leaching could be attributed to the removal of acidic and amorphous components (unhydrolyzed if any present) that might have adhered on the SNC surface and favoured enhanced coalescence among rubber particles and increased polymer-filler interaction.

The percentage retention in elongation at break (EB) of gum and SNC filled vulcanizates after leaching is displayed in **Figure 6**. It is obvious that, the percentage retention in elongation at break of filled vulcanizates increases with filler loading. This can be attributed to increased water absorption by the filler during leaching. Since the filler is highly hydrophilic in nature, the higher the filler content, the higher the water absorption. The increase in tension set (%) values of filled vulcanizates (particularly at higher filler loadings) also supports this observation. The improved elongation at break could be due to the increased interaction between latex and SNC. The increment in modulus with filler content (**Table 4**) and percentage retention in EB (after leaching) indicates

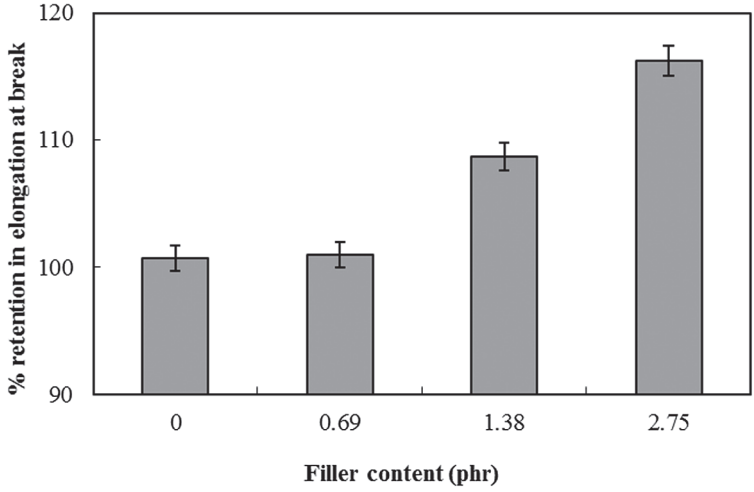

Figure 6 Percentage retention in elongation at break (EB) of SNC incorporated NR composites after leaching

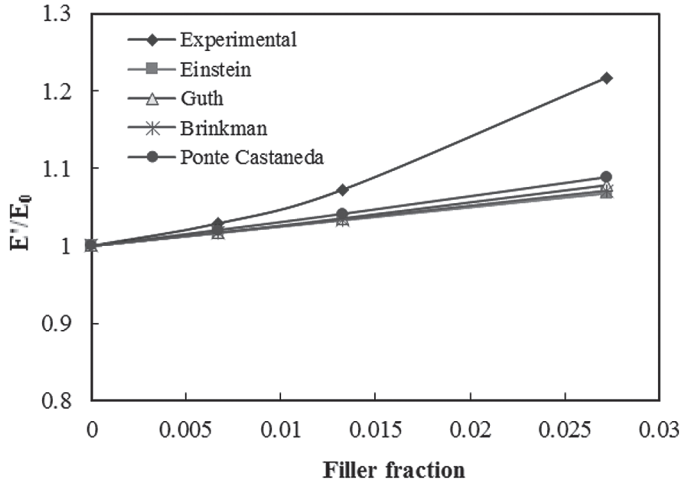

Figure 7 Theoretical modelling of the relative moduli of SNC incorporated NR composites

that the corn starch nanocrystals reinforce the latex vulcanizates without even losing elasticity.

The relative moduli (E'/E_0) of the composite films obtained from the experimental results were compared with theoretical predictions. The theoretical predictions are plotted with the experimental results in **Figure 7**. It can be seen that at higher filler loading, the modulus value calculated from the experimental results are higher than predicted. The difference in experimental result with the

theoretical assumptions at higher loadings indicates considerable interaction between polymer and filler [24].

CONCLUSIONS

Starch nanocrystals (SNC) were separated from modified corn starch by an acid hydrolysis method. The resulting corn starch crystal suspensions were characterized by DLS and XRD analysis and confirmed the presence of corn starch nanocrystals. Natural rubber latex–corn starch crystal nanocomposites were fabricated by a solution compounding method, and important vulcanizate properties measured such as swelling index and mechanical properties. An optimum SNC loading of 1.38 phr imparted improved solvent resistance capacity to the NR latex film. The mechanical properties of SNC incorporated vulcanizates were found to be good.

ACKNOWLEDGEMENTS

Anand K gratefully acknowledges the Rubber Research Institute of India (Rubber Board) for financial assistance in the form of a RRII Research Fellowship.

REFERENCES

1. LeCorre, D., Bras, J. and Dufresne, A., *Biomacromolecules,* **11** 1139–1153 (2010).
2. Whistler, R.L. and Paschall, E.F., *Starch: Chemistry and Technology*, New York, Academic Press (1965).
3. Lin, N., Huang, J., Chang, P. R., Anderson, D.P. and Yu, J., *J. of Nanomaterials,* **2011** 13 pages (2011).
4. www.starch.dk/ISI/market/index.asp
5. NPCS team, NIIR Project Consultancy Services (2014).
6. LeCorre, D., Bras, J. and Dufresne, A., *J. Nanopart. Res.,* **13** 7193–7208 (2011).
7. http://www.rubbernews.com/.
8. LeCorre, D., Bras, J. and Dufresne, A., *Macromol. Mater. Eng.,* **297** 969–978 (2012).
9. Angellier, H., Boisseau, S.M., Lebrun, L. and Dufresne, A., *Macromolecules,* **38(9)** 3783–3792 (2005).
10. Angellier, H., Boisseau, S. and Dufresne, A., *Macromolecules*, **38(22)** 9161–9170 (2005).
11. Tang, H., Qi, Q., Wu, Y., Liang, G., Zhang, L. and Ma, J., *Macromol. Mater. Eng*., **291** 629–637 (2006).
12. Xin, J, Wang, Y. and Liu, T., *Adv. J of Food Sc. and Technol.,* **4(5)** 270–276 (2012).
13. A.R. Payne, 'Dynamic properties of filler-loaded rubbers in Reinforcement of elastomers' G. Kraus (Ed.) Inter Science Publishers, chapter 3 (1965).

14. Bergstrom, J.S. and Boyce, M.C., *Rubber Chem. Technol.,* **72** 633–656 (1999).
15. Nguyen, D.D. and Dinh, K.M., *Vietnam J. of Mechanics*, *VAST,* **34(1)** 19–25 (2012).
16. Brinkman, H.C., *J. Chem. Phys.,* **20** 571 (1952).
17. LeCorre, D., Bras, J. and Dufresne, A., *Biomacromolecules,* **12** 3039–3046 (2011).
18. Hibi, Y., Matsumoto, T. and Hagiwara, S., *Cereal. Chem.,* **70(6)** 671–676 (1993).
19. Utrilla-Coello, R.G., Jaimes, C.H., Navas, H.C., Gonzalez, F., Rodriguez, E., Perez, L.A.B., Carterand, E.J.V. and Ramirez, J.A., *Carbohydrate Polymers,* **103** 596–602 (2014).
20. Song, S., Wang, C., Pan, Z and Wang, X., *J. Appl. Polym. Sci.,* **107** 418–422 (2008).
21. Beninca, C., Demiate, I.M., Lacerda, L.G., Filho, M.A.S.C., Ionashiro, M. and Schnitzler, E., *Ecl. Quim., Sao Paulo,* **33(3)** 13–18 (2008).
22. Jong, L. *Euro. Polym. J.*, **74** 136–147 (2016).
23. Claramma, N.M., *Ph. D. thesis,* Cochin University of Science and Technology (1997)
24. Selvin, T.P., Kuruvilla, J. and Thomas, S., *Mater Lett.,* **58** 281–289 (2004).